Ca^{2+} Dependency of Calpain 3 (p94) Activation†

Beatriz E. García Díaz,‡ Sherry Gauthier, and Peter L. Davies*

Department of Biochemistry and Protein Engineering Network of Centres of Excellence, Queen's University, Kingston, Ontario K7L 3N6, Canada

Received September 20, 2005; Revised Manuscript Received January 30, 2006

ABSTRACT: Calpain 3, commonly called p94 in the literature, is the abundant skeletal muscle-specific calpain that is genetically linked to limb girdle muscular dystrophy type 2A. Recently, we showed that p94's insertion sequence 1 (IS1) is a propeptide that must be autoproteolytically cleaved to provide access of substrates and inhibitors to the enzyme's active site. Removal of IS1 from the core of p94 by recombinant methods produced a fully active enzyme. Here we have resolved the discrepancies in the literature about the Ca^{2+} requirement of p94 using the protease core. Even at substoichiometric levels of Ca^{2+}, and in competition with EDTA, autoproteolyzed enzyme slowly accumulated. Because the initial autoproteolytic cleavage is an intramolecular reaction, transient binding of two Ca^{2+} ions to the core would be sufficient to promote the reaction that is facilitated by having the scissile peptide lying close to the active site cysteine. The second autolytic cleavage was much slower and required higher Ca^{2+} levels, consistent with it being an intermolecular reaction. Other metal ions such as Na^+, K^+, and Mg^{2+} cannot substitute for Ca^{2+} in catalyzing the intramolecular autoproteolysis of the p94 core or in the subsequent hydrolysis of exogenous substrates. These metal ions increase moderately the activity of this enzyme but only at very high concentrations. Thus, the proteolytic activity of the core of p94 and its deletion mutant lacking NS and IS1 was shown to be strictly Ca^{2+}-dependent. We propose a two-stage model of activation of the proteolytic core of p94.

Calpains comprise a large family of cytosolic Ca^{2+}-dependent cysteine proteinases with well-defined homologues present in vertebrates, invertebrates, and fungi (*1*, *2*). Genome sequencing projects have identified 14 calpain genes in humans, 13 in mice, four in *Drosophila*, 12 in *Caenorhabditis elegans*, two in fungi/yeast, and five in the unicellular organism *Trypanosoma brucei*, while only one gene has been found so far in plants (*Arabidopsis thaliana* and *Zea mays*). However, most of the calpains encoded by these genes have not yet been isolated from tissues or expressed in heterologous systems, and therefore, not much is known about their catalytic properties, the role of their specific domains, or the identity of their substrates and inhibitors. Much of what is known about this proteinase family has come from the characterization of two mammalian heterodimeric isoforms, μ- and m-calpain (also known as calpains 1 and 2, respectively). The three-dimensional structures of Ca^{2+}-free rat and human m-calpain were determined by X-ray crystallography (*3*, *4*) and showed clearly that these enzymes are enzymatically inactive in the absence of Ca^{2+} because the two domains (DI[1] and DII) of their catalytic core are misaligned by design. Binding of Ca^{2+} to the proteolytic core of μ-calpain (μI-II) results in a 50° rotation of DI relative to DII that ultimately aligns the active site residues in the right orientation for catalysis (*5*). Catalytic core domains I and II are common to all calpains, and the critical residues for binding of Ca^{2+} to these two domains are well-conserved. This suggests that the Ca^{2+}-dependent alignment of the active site is an intrinsic part of the activation mechanism of this protease family.

The muscle-specific calpain (designated as calpain 3, but traditionally known as p94) (*6*) has a domain organization similar to that of the μ- and m-calpain large subunits (54 and 51% identical, respectively). Although all the residues involved in binding of Ca^{2+} to the proteolytic core are absolutely conserved, there has been controversy in the literature about whether p94 is a Ca^{2+}-dependent protease. The main reason for this controversy is the failure to recover intact p94 from muscle extracts because it undergoes very rapid autolysis even in the presence of excess EDTA (*7*). Expression of recombinant p94 in COS cells also gave similar results (*7*). However, purified active p94 from insect cells exhibited Ca^{2+}-dependent autolysis (*8*).

The lack of stability of p94 has been attributed to the presence of its unique insertion sequences IS1 and IS2 (*9*) located within protease core DII and in the linker region

† This work was funded by the Heart and Stroke Foundation of Ontario, the Canadian Institutes for Health Research, and the Government of Canada's Network of Centres of Excellence program supported by the Canadian Institutes of Health Research and Natural Sciences and Engineering Research Council through PENCE (the Protein Engineering Network Centres of Excellence). P.L.D. holds a Canada Research Chair in Protein Engineering.

* To whom correspondence should be addressed: Department of Biochemistry and Protein Engineering Network of Centres of Excellence, Queen's University, Kingston, Ontario K7L 3N6, Canada. Telephone: (613) 533-2983. Fax: (613) 533-2497. E-mail: daviesp@post.queensu.ca.

‡ Present address: Division of Biochemistry, Department of Biological Sciences, University of Calgary, Calgary, Alberta T2N 1N4, Canada.

[1] Abbreviations: D, domain (as in DI, DII, DIII, and DIV); ICP-AES, inductively coupled plasma atomic emission spectrometry; Ni−NTA, nickel−nitrilotriacetic acid agarose; PEF, penta-EF-hand; SLY-MCA, succinyl-leucine-tyrosine-aminomethylcoumarin.

10.1021/bi051917j CCC: $33.50
Published on Web 02/23/2006

between DIII and DIV, respectively. Rapid autolysis of p94 is prevented by deletion of IS1 and IS2 (*7*), and some alternative splicing variants of p94 lacking these novel insertions have been found in different tissues (*7*, *10*−*15*). Lp82, a lens-specific splice variant of p94 that lacks N-terminal extension sequence NS and insertion sequences IS1 and IS2, has been detected as a full-length 82 kDa protein band in young rodent lenses, and the corresponding enzymatic activity band has been detected on casein zymograms (*16*). Introduction of IS1 into Lp82 destabilized the protein and caused a loss of enzymatic activity, whereas substitution of the shorter N-terminal sequence (AX1) present in Lp82 by NS or introduction of IS2 did not affect stability (*17*). These results strongly suggest that the stability and abundance of enzymatically active Lp82 in rodent lens extracts are due to the lack of IS1. Another alternatively spliced variant of mouse p94 that lacks IS1 and IS2 (p94:exon6^{-}-15^{-}16^{-}, p94Δ) has been successfully expressed in mammalian cells, and its proteolytic activity has been shown to be Ca^{2+}-dependent (*18*). Moreover, a new splicing variant of p94 lacking IS1 and the lysine-rich sequence in IS2 encoded by exon 15 has been isolated from human lymphocytes, and its enzymatic activity was also Ca^{2+}-dependent (*14*).

Although p94 undergoes rapid autolytic degradation during isolation and purification from muscle preparations, it has been found to be stable in intact skeletal muscle (*19*, *20*) or in saline-insoluble myofibrillar fractions (*21*). This apparent stability has been attributed to binding of p94 to connectin through the IS2 region. It is postulated that the high concentrations of NaCl used during purification result in dissociation of p94 from this stabilizing regulator and trigger Ca^{2+}-independent autolysis.

Unlike whole p94, the proteolytic core of p94 containing NS and IS1 can be produced in relatively large amounts in *Escherichia coli*, and the recombinant protein is fairly stable during purification (*22*). Using this truncated form of the enzyme, we have previously shown that the core of p94 is stable in EDTA but undergoes autolysis in the presence of Ca^{2+}. NS and IS1 are rapidly cleaved during this process at specific N-terminal sites by a strictly intramolecular reaction. We have also shown in recent studies that the IS1 region acts as an internal propeptide and that autoproteolytic removal of IS1 makes the activated enzyme available for hydrolysis of exogenous substrates and accessible to inhibitors (*23*). Here we have tried to resolve the discrepancies in the literature about the requirement for Ca^{2+} in the activation process and in its subsequent enzyme activity using the simplified protease core. Our results demonstrate that the catalytic core of p94 (p94I-II) and its deletion mutant lacking NS and IS1 (p94I-II ΔNS/ΔIS1) both require Ca^{2+} for activity. We also show that substoichiometric levels of Ca^{2+}, even in the presence of EDTA, support the gradual accumulation of autoproteolyzed enzyme, and this may be the root of the discrepancies in the literature about p94's Ca^{2+} requirement. However, other metal ions such as Na^{+}, K^{+}, and Mg^{2+} cannot substitute for Ca^{2+} in catalyzing the autoproteolysis of the p94 core or in priming hydrolysis of exogenous substrates, although they contribute measurable amounts of Ca^{2+} as impurities. These metal ions can increase the activity of this enzyme but only at unphysiologically high concentrations.

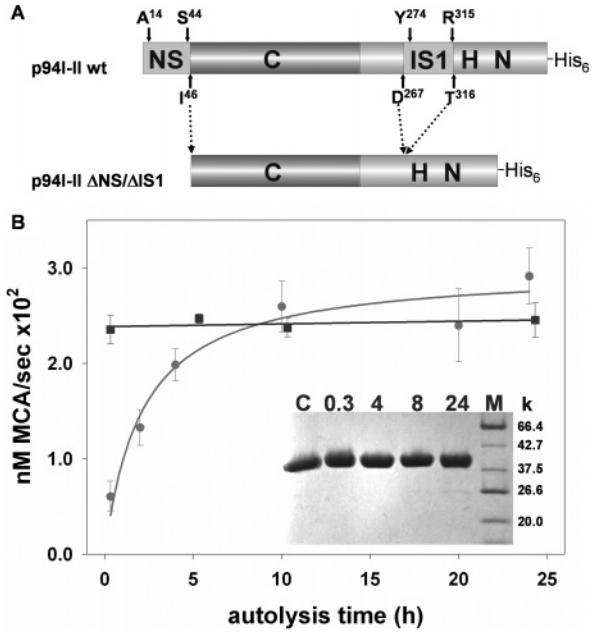

FIGURE 1: (A) Schematic representation of p94I-II deletion mutant p94I-II ΔNS/ΔIS1. Domains I and II are colored dark and light gray, respectively, and the positions of NS and IS1 sequences are indicated. The catalytic triad residues C, H, and N are shown at their locations in the enzyme. The residues in the P1 position of the autolytic sites identified by Rey and Davies (*22*) are indicated above p94I-II, and three significant residues in the deletion mutant are marked with dashed arrows. (B) Activity profile of p94I-II and p94I-II ΔNS/ΔIS1. Rates of hydrolysis of exogenous synthetic substrate SLY-MCA by p94I-II (●, light gray trace) and p94I-II ΔNS/ΔIS1 (■, dark gray trace) were measured at different times of preincubation in assay buffer containing 10 mM $CaCl_2$ (autolysis time). The inset in panel B corresponds to the SDS−PAGE analysis of p94I-II ΔNS/ΔIS1 incubation over the time frame of the experiment. Lanes are marked with the time of incubation (in hours). M refers to the molecular weight markers, and C represents an aliquot taken immediately after addition of Ca^{2+} but prior to addition of SLY-MCA.

EXPERIMENTAL PROCEDURES

Cloning, Mutagenesis, Expression, and Purification of Recombinant Proteins. The protease core of human calpain 3/p94 (p94I-II) and its active site knockout mutant, p94I-II C^{129}S, were prepared as previously described (*22*). These constructs contain NS and IS1 and are effectively a C-terminal truncation of p94 after Asp^{419} (Figure 1). A deletion mutant lacking both NS (residues 1−45) and IS1 (residues 268−315, inclusive) (Figure 1) was prepared by overlap extension PCR. Two PCRs were set up in parallel to amplify the 5′ fragment (encoding the region between NS and IS1, I^{46}−D^{267}, inclusive) and the 3′ fragment (encoding the C-terminal region after IS1, T^{316}−D^{419}, inclusive). For this purpose, two sets of primers were synthesized and each set had an external primer and an internal primer. The external primers encoded the new N-terminus and C-terminus, respectively, whereas each internal primer flanked the region upstream or downstream from the IS1. The internal primers were designed to generate PCR products with overlapping sequences at the junction site. The two new fragments were then pasted together in a third PCR using this overlapping region and the external primers. The final amplified product was ligated into the pET24a vector between the *Nde*I and *Xho*I sites to encode p94I-II ΔNS/ΔIS1 with a C-terminal hexahistidine tag (MI^{46}ISRN...CNLTAD^{419}LEH$_6$). The DNA

sequences of positive clones were verified. p94I-II ΔNS/ΔIS1 was expressed in *E. coli* BL21(DE3) under kanamycin selection. To make an inactive variant of the p94I-II ΔNS/ΔIS1, the active site Cys (C^{129}, numbering corresponds to full-length p94) was replaced with Ser using the single-stranded DNA method (*24*) and the same mutagenic primer previously designed for mutagenesis of p94I-II (*22*). The deletion construct and its active site knockout mutant (p94I-II C^{129}S ΔNS/ΔIS1) were purified according to the protocol previously described for p94I-II (*22*), but with size-exclusion Sephacryl S-200 chromatography included before the final Q-Sepharose FPLC step.

Autoproteolysis Assay. Autoproteolytic activity was measured by incubating p94I-II in 50 mM HEPES-NaOH (pH 7.6), 200 mM NaCl, 1 mM DTT, and varying added $CaCl_2$ concentrations (from 1 μM to 10 mM) at room temperature in a final volume of 200−500 μL at a protein concentration of 0.8 mg/mL (16 μM). Aliquots were removed at different times, and the reaction was stopped by addition of 3× SDS−PAGE sample buffer, 187.5 mM Tris-HCl (pH 6.8), 6% SDS, 30% glycerol, and 0.03% bromophenol blue. The progress of autolysis was analyzed by 10% SDS−PAGE and Coomassie blue staining. A control assay was carried out with 10 mM NaEDTA in place of Ca^{2+}. Similar autolysis experiments were carried out in the presence of different concentrations of monovalent (NaCl and KCl) and divalent ($MgCl_2$) metal ions. To prevent the existence of a background of Na^+ in the experiments in which the effects of monovalent metal ions on autolysis are compared, the buffer HEPES-NaOH was replaced with Tris-HCl, also at pH 7.6. We also tested p94I-II autolysis in the presence of a commercially available Ca^{2+}-free buffer purchased from Molecular Probes, Invitrogen (Calcium Calibration Buffer Kit 1), and in regular MilliQ H_2O.

Enzymatic Activity. The activity of p94I-II or p94I-II ΔNS/ΔIS1 against a 0.5 mM solution of the fluorogenic peptide substrate succinyl-leucine-tyrosine-aminomethylcoumarin (SLY-MCA) was assayed in 50 mM HEPES-NaOH (pH 7.6), 200 mM NaCl, 1 mM DTT, and 10 mM $CaCl_2$ at room temperature. MCA release was monitored over time (excitation at 360 nm and emission at 460 nm). To examine the effect of autolysis on the rate of SLY-MCA hydrolysis, p94I-II or p94I-II ΔNS/ΔIS1 (5 μM) was incubated in 50 mM HEPES-NaOH (pH 7.6), 200 mM NaCl, 1 mM DTT, and 10 mM $CaCl_2$. Aliquots were removed at different autolysis times and assayed for hydrolysis of SLY-MCA (0.5 mM). The initial rate of MCA release was calculated for each autolysis time point, and the degree of autolysis was analyzed by SDS−PAGE.

To determine the Ca^{2+} requirement for activity, we monitored the hydrolysis of SLY-MCA by p94I-II and p94I-II ΔNS/ΔIS1 at different Ca^{2+} concentrations (from 1 μM to 100 mM). Due to the effect of autolysis on the enzymatic activity of p94I-II, the enzyme was preincubated in assay buffer containing different $CaCl_2$ concentrations for 24 h prior to the assay to ensure that the extent of autolysis of each sample was only dependent on the Ca^{2+} concentration and not on the time of exposure.

The effect of different metal ions on the hydrolysis of SLY-MCA by p94I-II ΔNS/ΔIS1 was assayed in 50 mM Tris-HCl (pH 7.6), 1 mM DTT, and 10 mM $CaCl_2$ at room temperature. MCA release was monitored for 10−15 min after the addition of increasing concentrations of NaCl (from 50 mM to 1.6 M), KCl (from 50 mM to 1.4 M), and $MgCl_2$ (from 50 mM to 1.2 M). Choline chloride was used as a control for ionic strength (from 50 mM to 1.7 M). Initial rates of SLY-MCA hydrolysis were calculated for each concentration.

Digestion of m-Calpain C^{105}S by p94I-II and p94I-II ΔNS/ΔIS1. Proteolysis of the m-calpain C^{105}S heterodimer by p94I-II or p94I-II ΔNS/ΔIS1 was performed in 50 mM HEPES-NaOH (pH 7.6), 200 mM NaCl, 1 mM DTT, and 10 mM $CaCl_2$ at room temperature in a final volume of 250 μL. The enzyme:substrate molar ratio was 1:10 (0.5 mg/mL m-calpain C^{105}S and 0.025 mg/mL p94I-II or 0.02 mg/mL p94I-II ΔNS/ΔIS1; note that these two enzyme concentrations are equivalent in molar terms because of their different masses). In each case, the control reaction mixture contained 10 mM NaEDTA instead of $CaCl_2$. At specific time intervals (0.5, 4, 8, and 20 or 24 h), aliquots were removed and the reaction was stopped by addition of 3× SDS−PAGE sample buffer. The progress of proteolytic digestion was analyzed by SDS−PAGE using a 10% gel. In a control experiment, the m-calpain C^{105}S heterodimer substrate was incubated in the same buffer but without enzymes to show that this inactive variant of m-calpain does not autolyse or break down during the long exposure to $CaCl_2$.

Intrinsic Tryptophan Fluorescence Measurements. We monitored conformational changes induced by binding of Ca^{2+} to p94I-II and its mutants by measuring changes in the intrinsic tryptophan fluorescence in a Perkin-Elmer LS50B fluorescence spectrophotometer. The data were collected at 23 °C in the same buffer used for SLY-MCA hydrolysis experiments. Excitation and emission wavelengths were set at 280 and 340 nm, respectively. To eliminate any possible complications due to autolysis, the inactive mutants, p94I-II C^{129}S and p94I-II C^{129}S ΔNS/ΔIS1, were used in these assays. The protein concentration was 1 μM. $CaCl_2$ (50 mM) dissolved in reaction buffer was continuously pumped into the cuvette at a flow rate of 4 μL/min while the reaction was vigorously stirred using the internal magnetic stirrer of the fluorimeter. The recorded fluorescence intensity values were corrected for dilution, and the normalized data were fitted to the Hill equation, $y = x^n/(k^n + c^n)$, where y is the fraction of maximal intensity change, $x = [Ca^{2+}]$, $k = [Ca^{2+}]_{0.5}$, which is the value of $[Ca^{2+}]$ at which fluorescence intensity reaches a half-maximal value, and n is the Hill coefficient.

Determination of Ca^{2+} Levels in Stock Solutions. The levels of Ca^{2+} contamination present in 1 M NaCl, 1 M KCl, and 1 M $MgCl_2$ stock solutions and MilliQ water were determined by elemental analysis at the Analytical Laboratory for Environmental Science Research and Training (Analest), University of Toronto (Toronto, ON), using inductively coupled plasma atomic emission spectrometry (ICP-AES).

RESULTS

A Deletion Mutant of p94I-II Lacking NS and IS1 Is Active in the Presence of Ca^{2+}. The rapid autolytic degradation of calpain 3 (p94) has hampered many efforts to isolate, purify, and characterize this enzyme. Using a truncated version of the enzyme that comprises proteolytic core domains I and

II and two of the three unique sequences of p94, NS and IS1, we have previously shown that two initial, very rapid autolytic cleavages occur at the N-termini of NS and IS1 in a strictly intramolecular manner (*22*). Over a period of hours, a second autolytic cleavage at the C-termini of both NS and IS1 removes NS and cuts out the internal IS1 fragment. We have recently shown that IS1 serves as an internal propeptide and its autolytic release causes activation of the proteolytic core of p94 (*23*). To confirm this idea, we have prepared a double deletion mutant of p94I-II that lacks NS and IS1 (p94I-II ΔNS/ΔIS1) and have evaluated its activity toward a synthetic calpain substrate SLY-MCA.

The deletion mutant lacks the first 45 residues corresponding to NS, and the region from D^{268} to R^{315}, inclusive, encompassing IS1 (Figure 1A), and therefore does not have the autolytic cleavage sites identified previously (*22*). Although the expression levels are not as high as those obtained for p94I-II, this variant is produced in soluble form in *E. coli* and is stable during the four consecutive chromatographic purification steps to yield a homogeneous protein sample (Figure 1B, lane C in inset).

When p94I-II ΔNS/ΔIS1 (5 μM) was assayed against the small synthetic calpain substrate SLY-MCA in the absence of Ca^{2+}, no formation of MCA was observed. However, when $CaCl_2$ (10 mM) was added to the reaction mixture, MCA release over time was apparent and initial reaction rates (Figure 1B, ■, dark gray trace) were similar to the maximal activity levels reached by p94I-II (5 μM) after autolysis for several hours (Figure 1B, ●, light gray trace) (*23*). In contrast to p94I-II, the activity of p94I-II ΔNS/ΔIS1 did not increase upon incubation with $CaCl_2$ for 24 h but remained constant over this extended period of time. Indeed, the plateau activities of the naturally autolysed enzyme and the recombinant equivalent (p94I-II ΔNS/ΔIS1) were not significantly different at the 24 h time point. p94I-II ΔNS/ΔIS1 did not undergo autolytic degradation in the presence of Ca^{2+} during this time as shown by SDS−PAGE (Figure 1B, inset).

Ca^{2+} Requirement of p94I-II and Its Deletion Mutant p94I-II ΔNS/ΔIS1 for Enzymatic Activity on Exogenous Substrates. To measure the concentration of Ca^{2+} required for half-maximal activity, SLY-MCA hydrolysis by p94I-II or p94I-II ΔNS/ΔIS1 was assayed at different Ca^{2+} levels. At low Ca^{2+} concentrations (from 5 μM to 0.5 mM), the plot of initial rates of SLY-MCA hydrolysis versus Ca^{2+} concentration for both p94I-II and p94I-II ΔNS/ΔIS1 exhibited a sigmoidal shape (Figure 2). The data fit readily to the Hill equation (Hill coefficient $n = 2.01$ for p94I-II and $n = 1.97$ for p94I-II ΔNS/ΔIS1), suggesting that Ca^{2+} binding is a cooperative process and that it involves two sites. Half-maximal activity values were reached at approximately 150 and 90 μM $CaCl_2$ for p94I-II and p94I-II ΔNS/ΔIS1, respectively (Figure 2). Addition of more $CaCl_2$ beyond 0.5 mM resulted in a hyperbolic increase in activity (not shown), as observed with the protease core of μ-calpain (*5*). Binding of Ca^{2+} to p94I-II and its deletion mutant was also monitored by intrinsic tryptophan fluorescence (Figure 2, inset). The active site knockout mutants (p94I-II $C^{129}S$ and p94I-II $C^{129}S$ ΔNS/ΔIS1) were used in these experiments to avoid any possibility of autolysis. A sigmoidal increase in fluorescence with an increase in Ca^{2+} concentration was observed, and similar values for $[Ca^{2+}]_{0.5}$ and Hill coefficients (n) were estimated (Figure 2, inset), suggesting that cooperative Ca^{2+} binding induces a conformational change in the proteolytic core of p94.

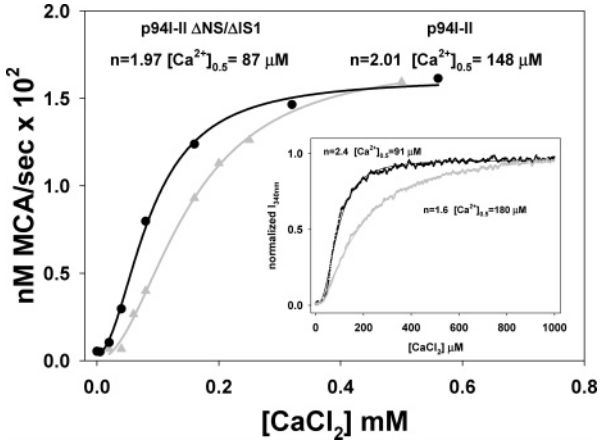

FIGURE 2: Ca^{2+}-dependent protease activity of p94I-II and p94I-II ΔNS/ΔIS1. Initial rates for SLY-MCA hydrolysis by p94I-II (gray trace and triangles) and p94I-II ΔNS/ΔIS1 (black trace and circles) at varying Ca^{2+} concentrations were fitted to the Hill equation plot. The estimated values for the Hill coefficient (n) and the Ca^{2+} concentration for half-maximal activity ($[Ca^{2+}]_{0.5}$) for p94I-II and p94I-II ΔNS/ΔIS1 are indicated. Ca^{2+}-induced conformational change was followed by intrinsic tryptophan fluorescence (at 340 nm) of p94I-II $C^{129}S$ (gray trace) and p94I-II $C^{129}S$ ΔNS/ΔIS1 (black trace) at varying Ca^{2+} concentrations (inset). The Hill equation was fitted (solid lines) to a semilogarithmic plot of the normalized fluorescence intensity values (dotted curves).

To determine if the Ca^{2+} requirement for hydrolysis of a small synthetic substrate applied equally well to large natural protein substrates, we assayed the proteolytic activity of p94I-II and p94I-II ΔNS/ΔIS1 against m-calpain. We used m-calpain $C^{105}S$, an inactive mutant of m-calpain that is incapable of autoproteolysis, because it is readily digested by the analogous proteolytic core of μ-calpain (μI-II) (*5*). p94I-II and p94I-II ΔNS/ΔIS1 were mixed with m-calpain $C^{105}S$ at an enzyme:substrate molar ratio of 1:10 in the presence of 10 mM $CaCl_2$ or 10 mM NaEDTA. Although the activities of p94I-II and p94I-II ΔNS/ΔIS1 were comparably weak, digestion products of the m-calpain $C^{105}S$ large subunit (80K) were clearly formed when Ca^{2+} was present (Figure 3A,B). Two main bands with approximate molecular weights of 55K and 24K were detected after incubation for 4 h in Ca^{2+} and continued to accumulate during the next 20−24 h. In contrast, no m-calpain digestion products were observed after incubation for 20−24 h in NaEDTA. When m-calpain $C^{105}S$ was digested with p94I-II, the 48K enzyme band disappeared during the incubation while its typical autolytic products (30K, 26K, 17K, and 13K) appeared in addition to the above-mentioned 55K and 24K m-calpain digestion products (Figure 3B). The m-calpain $C^{105}S$ heterodimer (80K and 21K bands) alone remained stable during a 24 h incubation in 10 mM $CaCl_2$ (Figure 3C), indicating that the 55K and 24K digestion fragments are the result of Ca^{2+}-dependent specific cleavages by the proteolytic core of p94 in its active form. In this regard, p94I-II ΔNS/ΔIS1 was slightly more active than p94I-II (Figure 3A,B), possibly because the latter is inactive until it undergoes autoproteolysis, and even then, intermolecular autoproteolysis may compete with proteolysis of the exogenous substrate.

Effect of Ca^{2+} and Other Metal Ions on Autolysis of p94I-II. Rapid autolytic degradation of full-length p94 during

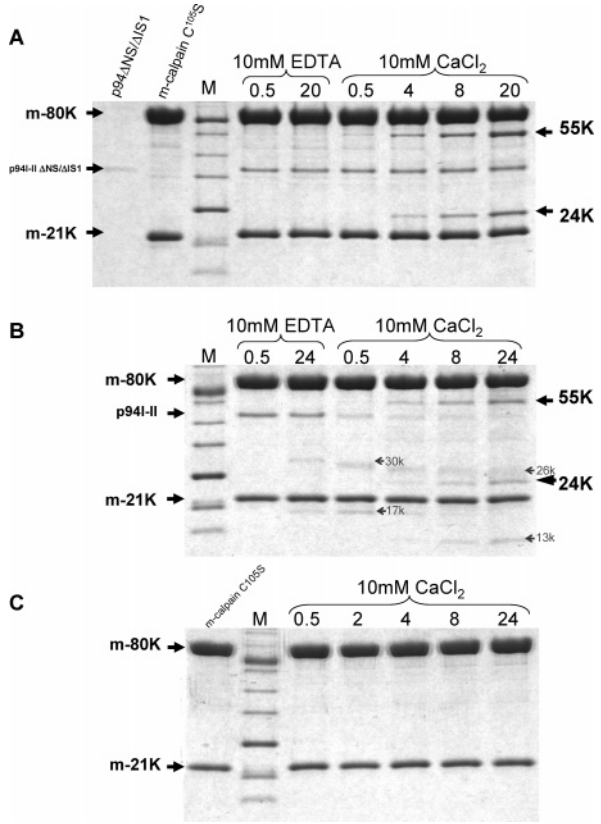

FIGURE 3: SDS−PAGE analysis of digestion of m-calpain by p94I-II and p94I-II ΔNS/ΔIS1. Proteolysis of the inactive m-calpain heterodimer (m80K/21K $C^{105}S$) by p94I-II ΔNS/ΔIS1 (A) and p94I-II (B) was performed at an enzyme:substrate molar ratio of 1:10 in the presence of 10 mM $CaCl_2$ and in a control reaction mixture containing 10 mM NaEDTA instead of $CaCl_2$. The inactive m-calpain $C^{105}S$ heterodimer was separately incubated in the presence of 10 mM $CaCl_2$ to assess autolysis in the absence of exogenous enzyme (C). Aliquots of each of the reaction mixtures in $CaCl_2$ were taken at different time points (lanes 6−9 in panel A, lanes 4−7 in panel B, and lanes 3−7 in panel C) and of the reaction mixture in EDTA (lanes 4 and 5 in panel A and lanes 2 and 3 in panel B). For comparison, purified p94I-II ΔNS/ΔIS1 and m-calpain $C^{105}S$ were loaded on the gel shown in panel A (lanes 1 and 2, respectively), and m-calpain $C^{105}S$ was loaded on the gel shown in panel C (lane 1). Lane M in each panel contained molecular weight markers (from top to bottom, 66.4K, 55.5K, 42.7K, 37.5K, 26.6K, 20.0K, and 14.3K). Bands corresponding to p94I-II ΔNS/ΔIS1 (38K), p94I-II (48K), and the large (m80K) and small (m21K) subunits of inactive m-calpain are shown by arrows at the left. The digestion fragments produced during the reaction (55K and 24K) and the autolytic fragments of p94I-II (30K, 26K, 17K, and 13K) are indicated by arrows at the right.

extraction from muscle preparations or expression in heterologous systems even in the presence of EDTA has been the reason for discrepancies in the literature about the Ca^{2+} dependency of this calpain isoform. Some reports have suggested that even though p94 is stable in intact skeletal muscle (*19*, *20*) or in their saline-insoluble myofibrillar fractions (*21*), rapid degradation of p94 takes places when NaCl is used in extraction or purification procedures. We have previously shown that p94I-II rapidly autolyses in 10 mM Tris-HCl (pH 7.6), 10 mM DTT, and 10 mM $CaCl_2$ but does not break down in this time frame when it is incubated in 10 mM Tris-HCl, 10 mM DTT, and 10 mM NaEDTA (*22*). To evaluate whether the presence of other metal ions can substitute for Ca^{2+} in triggering autolysis, we incubated p94I-II in buffers containing different concentrations of NaCl, KCl, $MgCl_2$, and $CaCl_2$, as well as EDTA.

When p94I-II (16 μM) was incubated for 30 min in 50 mM HEPES-NaOH (pH 7.6), 200 mM NaCl, 10 mM DTT, and 10 mM NaEDTA, no digestion was observed. After 24 h, a trace amount of cleavage was noticeable as faint bands with approximate molecular weights of 30K and 17K (Figure 4A). We have previously identified these bands to be the product of the early autolytic cleavage sites after Ala^{14} and Tyr^{274} (*22*). When very low, substoichiometric $CaCl_2$ concentrations (<20 μM) were added, formation of these cleavage products was dramatically improved (Figure 4B). The late autolytic cleavages, characterized by cuts at Ser^{44} and Arg^{315} (*22*) and formation of cleavage products with molecular weights of 26K and 13K, were not detected in the presence of EDTA and were only represented by a very faint 26K band at substoichiometric Ca^{2+} concentrations. However, at Ca^{2+} concentrations of ≥20 μM, the late autolysis products (26K and 13K) became more evident in our SDS−PAGE analysis. At Ca^{2+} concentrations between 20 μM and 10 mM, the extent of this second phase was directly proportional to the amount of Ca^{2+} present in the reaction mixture (Figure 4B).

To assess the effect of other metal ions on autolysis, we incubated p94I-II (16 μM) in 50 mM Tris-HCl (pH 7.6), 1 mM DTT, 10 mM NaEDTA, and 200 mM MeCl (with MeCl being NaCl, KCl, or $MgCl_2$) for 24 h and evaluated the extent of autolysis by SDS−PAGE. Figure 5A shows that traces of initial autolytic cleavage are barely detectable in the control (no salt added) and in the presence of KCl or $MgCl_2$. In the presence of 200 mM NaCl, a slightly enhanced autolysis was seen. Panel B of Figure 5 shows that the effect of NaCl appears to be concentration-dependent. This was corroborated when samples incubated in Tris-HCl buffer without NaCl did not show signs of autolysis, whereas when the enzyme was incubated in HEPES-NaOH buffer without or with 200 mM NaCl, traces of autolysis were recorded. Interestingly, no traces of autolysis were seen when equal concentrations of the enzyme were incubated for 24 h in a commercially available Ca^{2+}-free buffer (Molecular Probes, Invitrogen), but faint autolytic bands were apparent when p94I-II was simply incubated in MilliQ water for the same period of time. It is worth noting that in no case did incubation with metal ions other than Ca^{2+} give rise to the second autolytic event. Furthermore, the extent of autolysis seen after incubation in 200 mM NaCl for 24 h was still much lower (2−5%, estimated by eye) than that observed with even substoichiometric amounts of Ca^{2+} (∼40−50%, again estimated by eye), and it was comparable with the levels of autolysis recorded when the sample was incubated in MilliQ H_2O.

Effect of Ca^{2+}, Na^+, K^+, and Mg^{2+} on SLY-MCA Hydrolysis by p94I-II ΔNS/ΔIS1. To complete this study, we tested the effect of different metal ions on enzymatic activity toward the synthetic substrate SLY-MCA. Since hydrolysis of SLY-MCA did not occur in the absence of Ca^{2+}, the effect of Na^+, K^+, and Mg^{2+} on p94I-II ΔNS/ΔIS1 activity was assessed by adding increasing concentrations of these metal ions to the reaction mixture containing 10 mM $CaCl_2$ (Figure 6). As a comparison, the effect of increasing Ca^{2+} concentrations on the hydrolysis rate was included in the analysis on the same scale. Comparable choline chloride concentrations

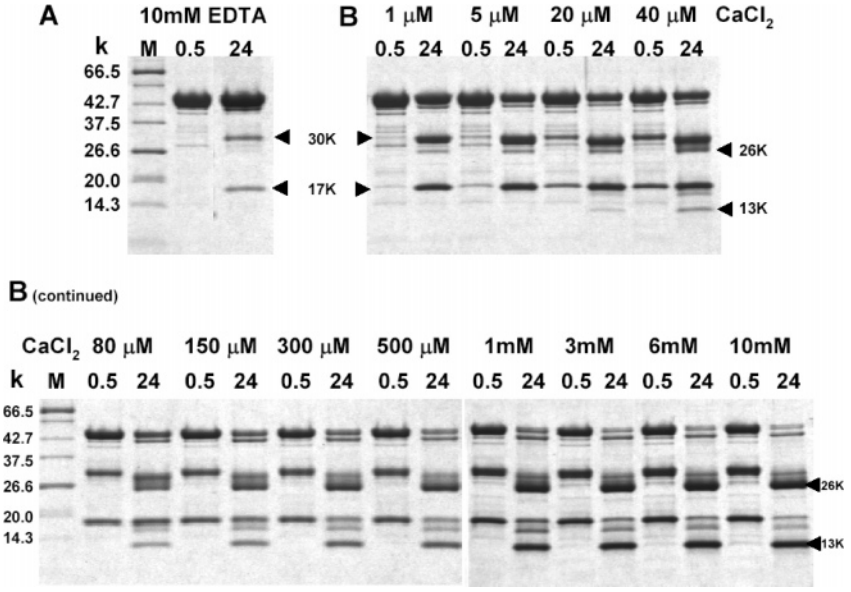

FIGURE 4: Ca^{2+}-dependent autolysis of p94I-II. p94I-II (16 μM) was incubated in 50 mM HEPES-NaOH (pH 7.6) buffer containing $CaCl_2$ concentrations ranging from 1 to 40 μM (B, top right panel) and from 80 μM to 10 mM (B, bottom panel). The approximate Na^+ ion concentration in the buffer is 25 mM, and this would contribute >0.2 μM Ca^{2+} from reagent impurities. For each Ca^{2+} concentration, aliquots were taken at 0.5 and 24 h. A control reaction mixture containing 10 mM NaEDTA instead of $CaCl_2$ is shown alongside the molecular weight markers (M) in panel A. Autolytic fragments at 30K, 26K, 17K, and 13K are indicated by arrowheads.

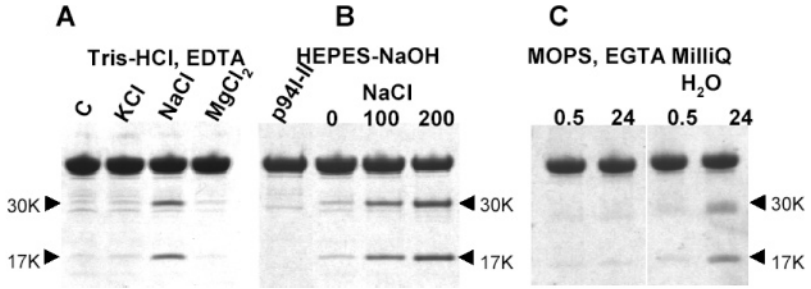

FIGURE 5: Effect of Na^+, K^+, and Mg^{2+} on p94I-II autolysis. p94I-II (16 μM) was incubated for 24 h in 50 mM Tris-HCl (pH 7.6) and 10 mM NaEDTA without salt (C) or 200 mM KCl, NaCl, or $MgCl_2$ (panel A) or in 50 mM HEPES-NaOH (pH 7.6) containing 0, 100, and 200 mM NaCl (panel B). An aliquot of the enzyme prior to incubation was loaded for comparison (p94I-II). As control reactions, p94I-II (16 μM) was incubated for 0.5 and 24 h in 30 mM MOPS buffer (pH 7.2), 10 mM K_2EGTA, 100 mM KCl (calcium-free buffer, Molecular Probes), and MilliQ H_2O (panel C).

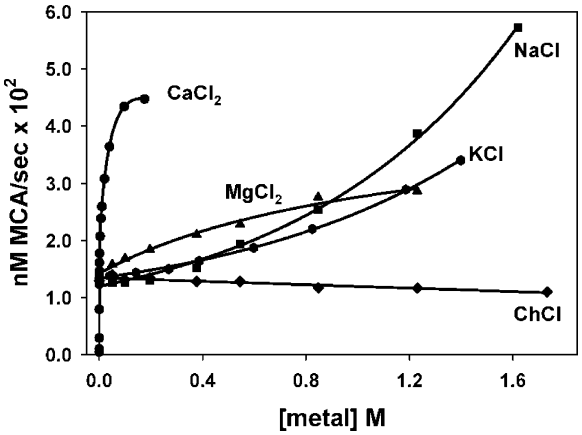

FIGURE 6: Effect of Ca^{2+}, Na^+, K^+, and Mg^{2+} on enzymatic activity of p94I-II ΔNS/ΔIS1. SLY-MCA hydrolysis was assayed in buffer containing 10 mM $CaCl_2$ at increasing concentrations of NaCl (■), KCl (●), $MgCl_2$ (▲), or $CaCl_2$ (●). Increasing concentrations of choline chloride were added in a control experiment for ionic strength and volume increase (◆).

were used in a separate assay as a control for ionic strength and volume increase. Figure 6 shows that the rate of hydrolysis was dramatically increased when the Ca^{2+} concentration was increased from 10 to 100 mM, whereas 10-fold higher concentrations of Na^+, K^+, or Mg^{2+} produced a moderate, much smaller increase in the rate of hydrolysis.

Endogenous Ca^{2+} Levels in Stock Solutions. Finally, we investigated whether the slight autolysis observed in the presence of metal ions such as Na^+, K^+, and Mg^{2+} could be due to traces of $CaCl_2$ in the solutions used in these assays. Direct measurement of Ca^{2+} levels was carried out at the Analytical Laboratory for Environmental Science Research and Training (Analest), University of Toronto, using ICP-AES. The results obtained showed that our 1 M NaCl stock solution contained 5.6 μM Ca^{2+}, whereas the 1 M KCl and 1 M $MgCl_2$ stock solutions contained 0.74 and 0.78 μM Ca^{2+}, respectively. The level of Ca^{2+} contamination in Milli Q water was below the detection limit (0.002 mg/L). Therefore, the "endogenous" Ca^{2+} level present in our autolysis assays performed in buffer containing 200 mM NaCl was approximately 1 μM, whereas the assays carried out in 200 mM KCl or 200 mM $MgCl_2$ contained only ~150 nM Ca^{2+}.

DISCUSSION

The rapid autolysis of p94 during extraction from skeletal muscle even in the presence of excess EDTA (*7*) has led to

controversy in the literature about whether p94 is a strictly Ca^{2+}-dependent protease. The fact that p94 shares an overall level of sequence identity of 54 and 51% with the large subunits of μ- and m-calpain, respectively, and that the residues involved in Ca^{2+} coordination in the protease core and PEF domain IV are strictly conserved between these isoforms strongly suggests that the proteolytic activity of p94 is also regulated by Ca^{2+}-dependent mechanisms. In this study, we have attempted to resolve the discrepancies in the literature about the requirement for Ca^{2+} in the activation process and postactivation using the simplified p94 protease core and a deletion variant that lacks NS and IS1.

We have recently shown that the enzymatic activity of both p94I-II and its N-terminal deletion mutant lacking NS (p94I-II ΔNS) toward the synthetic substrate SLY-MCA increases with the time of incubation in buffer containing $CaCl_2$ and reaches a plateau value after several hours (*23*). This Ca^{2+}-dependent activation process correlates with the progression of autolysis and led us to the conclusion that IS1 functions as an internal propeptide that blocks the active site until the first intramolecular cleavage is made, after which the cleft is opened to substrates and inhibitors (Figure 7). We also demonstrated that full activation is reached after a second cleavage that takes place much later (after ca. 10 h) and releases the propeptide. Consistent with our hypothesis, the enzymatic activity of the double deletion mutant p94I-II ΔNS/ΔIS1 toward SLY-MCA was shown to be similar to the maximal activity levels reached by an equal quantity of p94I-II after autolysis for several hours. Importantly, these levels of activity did not change over a 24 h period of exposure to $CaCl_2$, during which the double deletion mutant was stable and did not autolyse. This stability was to be expected since the deletion mutant lacks the autolytic cleavage sites present in p94I-II. As in the case of p94I-II, the activity levels of p94I-II ΔNS/ΔIS1 are much lower than the ones recorded for the proteolytic core of μ-calpain (μI-II) toward substrates such as SLY-MCA with an estimated 5-fold higher K_m value and a 40−50-fold lower k_{cat} value at 10 mM $CaCl_2$. The specific caseinolytic activity of a full-length p94 variant lacking insertion sequences 1 and 2 (p94Δ) was recently determined to be ~80-fold lower than that of recombinant m-calpain (*18*). Although it is not possible to directly compare the activity values of p94Δ with the ones determined by us for p94I-II and p94I-II ΔNS/ΔIS1, these reports taken together with our findings suggest that p94 has evolved to be an enzyme that is less active than the ubiquitous calpains, at least toward exogenous substrates. Despite the weak activity displayed by p94I-II and its deletion mutant, their stability provided greatly simplified proteases with which we studied several aspects of p94 activation and regulation by Ca^{2+}.

The plots of enzymatic activity versus Ca^{2+} concentration for both p94I-II and the double deletion mutant exhibited a sigmoidal shape suggesting cooperative binding of Ca^{2+} to the core of p94. Moreover, binding of Ca^{2+} to these two forms of the p94 core is accompanied by a conformational change as shown by the sigmoidal increase in the intrinsic tryptophan fluorescence. Similar results have been reported for the proteolytic core of μ- and m-calpain (μI-II and mI-II, respectively) (*5*, *25*). The sigmoidal characteristics of the Ca^{2+} titration curves (for both activity and intrinsic tryptophan fluorescence) are very similar to the ones determined

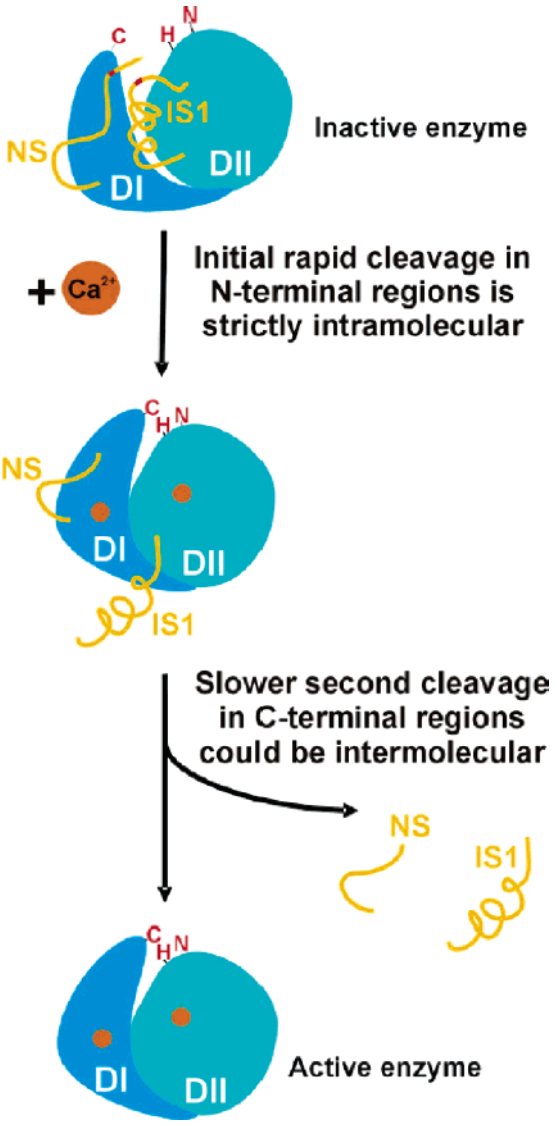

FIGURE 7: Model of activation of the proteolytic core of p94. Activation of p94 by Ca^{2+} occurs in two stages. The first stage begins with the realignment of the catalytic triad (residues colored red) into an active conformation upon binding of Ca^{2+} (orange balls) to domains I (blue) and II (cyan). This is accompanied by a significant conformational change of the proteolytic core that is emblematic of the proteolytic cores of μ- and m-calpain. The first stage is completed with the rapid intramolecular cleavages in the N-termini of NS and IS1 (scissile bonds colored red). This occurs immediately upon binding of Ca^{2+}. The second stage is the autolytic cleavage at the C-terminal ends of NS and IS1 (colored gold). This step, much slower and presumably intermolecular, renders the enzyme fully active (while Ca^{2+} is present) due to the autolytic removal of the internal propeptide (IS1).

for the homologous μ- and m-cores with comparable values for the Hill coefficient ($n \sim 2$). Crystallographic studies of μI-II and mI-II confirmed two non-EF-hand Ca^{2+} binding sites, one in domain I and the second in domain II (*5*, *25*). The residues involved in Ca^{2+} coordination at these two sites are strictly conserved in the proteolytic core of p94, and therefore, it should not be surprising that the Ca^{2+} dependency of p94 lies, as in the case of μ- and m-calpain, in the proteolytic core.

The Ca^{2+} requirement for half-maximal activity of p94I-II (~150 μM) and p94I-II ΔNS/ΔIS1 (~90 μM) lies between the values reported for μI-II (~40 μM) (*5*) and the active mutant of mI-II, mI-II $G^{203}A$ (~180 μM) (*25*). The latter

two protease cores have Ca^{2+} requirements similar to those of their full-length counterparts (~25 and 325 μM, respectively) (*26*). A splice variant of p94 lacking IS1 and the lysine-rich region of IS2 present in lymphocytes showed a $[Ca^{2+}]_{0.5}$ of ~20−30 μM (*14*). This result is similar in magnitude to the $[Ca^{2+}]_{0.5}$ value calculated here for p94I-II ΔNS/ΔIS1 (~90 μM). However, the Ca^{2+} requirement for half-maximal activity of p94Δ (full-length p94 lacking IS1 and IS2) has been determined recently by another group to be much higher (pCa = 2.9, i.e., $[Ca^{2+}]$ ~ 1 mM) (*18*) than the value we estimated for the proteolytic core of p94 in isolation. This large difference in the Ca^{2+} requirement (~10-fold) cannot be attributed to the lack of domains III and IV in our simplified protease core construct since the presence of these domains in the lymphocyte p94 variant does not seem to increase its Ca^{2+} requirement. In fact, it is very difficult to explain the 50-fold difference in the Ca^{2+} requirement of these two p94 splice variants (*14*, *18*), considering that they differ by only the small region of IS2 encoded by exon 16.

Two distinct methods revealed that p94I-II has an almost 2-fold higher Ca^{2+} requirement than its mutant lacking both NS and IS1. Since the intrinsic tryptophan fluorescence studies were carried out with inactive mutants (p94I-II $C^{129}S$ and p94I-II $C^{129}S$ ΔNS/ΔIS1) that are unable to autolyse, these results suggested that the difference in Ca^{2+} requirement observed here was not due to artifacts introduced by autoprocessing of the enzyme but to intrinsic characteristics of p94I-II. The fluorescence curves of p94I-II and p94I-II ΔNS/ΔIS1 were identical to those of their active site knockout mutants (data not shown). Furthermore, the mutant p94I-II ΔNS exhibited $[Ca^{2+}]_{0.5}$ values similar to those of p94I-II (data not shown). Thus, we hypothesize that the presence of IS1 is responsible for the higher Ca^{2+} requirement observed for p94I-II. In a previous study, we modeled IS1 as an internal propeptide that is blocking the active site from substrates and inhibitors (*23*). An α-helical region in IS1 was suggested to be the steric hindrance that causes the silencing of this enzyme. Therefore, it is conceivable that the presence of IS1 interferes with the cooperative Ca^{2+} activation mechanism involving domains I and II described by Moldoveanu et al. (*5*). However, in the absence of a structure for p94, the basis for this difference remains somewhat speculative.

The Ca^{2+} dependency of the p94 core is not restricted to its action on small synthetic substrates. Although digestion of recombinant m-calpain $C^{105}S$ by p94I-II and p94I-II ΔNS/ΔIS1 was very slow, the appearance of two proteolytic fragments (55K and 24K) was observed only in the presence of Ca^{2+} and was not the result of nonspecific m-calpain $C^{105}S$ breakdown during the long incubation time in $CaCl_2$. A similar band pattern was observed for digestion of m-calpain $C^{105}S$ by μI-II (*5*). However, in the latter case, the reaction was faster and the proteolytic fragments started to accumulate during the first 20 min after Ca^{2+} addition.

Taken together, these results show that Ca^{2+} is required for p94 proteolytic activity. Other metal ions such as Na^+, K^+, and Mg^{2+} were not able to support the hydrolysis of SLY-MCA or the proteolytic digestion of m-calpain $C^{105}S$ in the absence of Ca^{2+} (not shown). When added at very high concentrations in the presence of sufficient Ca^{2+}, they produced a moderate increase in the initial rates of SLY-MCA hydrolysis. A comparable effect has been published for μI-II (*5*), and it has been attributed to a nonspecific stabilizing effect of these metal ions on the structure of the proteolytic core, which possibly replaces some of the electrostatic interactions present in the full-length enzymes.

The rapid autolysis of p94 has been attributed to its two unique insertion sequences, IS1 and IS2, present in p94 but not in μ- or m-calpain (*7*). While several alternative splice variants of p94 lacking these sequences have been identified as intact enzymes in different tissues and their proteolytic activity has been shown to be Ca^{2+}-dependent (*10*, *14*, *18*), intact p94 has not been successfully extracted from skeletal muscle preparations. Even in the presence of EDTA, autolytic fragments are produced and accumulate over the course of extraction and purification (*7*). A similar degradation occurs when p94 is produced recombinantly in mammalian cells (COS cells) (*7*).

In our study, extremely low, substoichiometric Ca^{2+} concentrations (1−20 μM) were sufficient to catalyze the first autolytic step to a large extent (~40−50%, estimated by eye), suggesting that the first autolytic cleavage occurs very rapidly, possibly because the peptide bond that is cleaved is located very close to the active site cysteine, which is in agreement with our previously reported model (*23*). Following this reasoning, we hypothesized that the very slight autolysis observed in the presence of relatively high concentrations (100−200 mM) of other metal ions such as Na^+, K^+, and Mg^{2+} could be the effect of traces of $CaCl_2$ in the solutions used in these assays. We subsequently corroborated the presence of Ca^{2+} in these solutions. The endogenous Ca^{2+} concentrations were determined to be 5.6, 0.74, and 0.78 μM Ca^{2+} in our 1 M NaCl, 1 M KCl, and 1 M $MgCl_2$ stock solutions, respectively. Our hypothesis is further supported by the lack of autolysis seen when the enzyme was incubated in a commercially available Ca^{2+}-free buffer containing EGTA, which is known to be a better chelator for Ca^{2+}. The fact that traces of autolysis can be seen even in MilliQ water suggests that the low levels of Ca^{2+} present in glass and plasticware, water, and reagents are sufficient to allow this first autolytic step. Even in the presence of excess EDTA, competition for Ca^{2+} between the chelating agent and the enzyme could be taking place over the extended period of 24 h. Presumably, whenever a molecule of p94I-II simultaneously binds two Ca^{2+} ions at the cooperative sites in DI and DII, irreversible cleavage occurs and the early autoproteolytic cleavage products (30K and 17K) slowly accumulate. Although sporadic, these occasional autolytic events are favored kinetically by the ideal position of the scissile peptide bond close to the nucleophilic thiol group (Figure 7). Autolysis at the C-terminal sites and hydrolysis of exogenous substrates such as SLY-MCA do not possess this kinetic advantage and, therefore, would be less susceptible to these infrequent events. The minor enhancement seen when relatively large concentrations of NaCl were added to the autolysis reaction could partly be due to larger amounts of contaminating Ca^{2+} in our NaCl (as compared to KCl or $MgCl_2$) in addition to the stabilizing effect of metal cations on the structure of the p94 proteolytic core through electrostatic interactions discussed above. The work of Branca et al. (*8*) with purified full-length p94 produced in insect cells supports this hypothesis. Rapid accumulation of autolytic products was detected when this purified enzyme was

incubated in substoichiometric amounts of free Ca^{2+} (submicromolar range).

Figure 7 summarizes our model for the activation mechanism of the proteolytic core of p94. Activation occurs in two steps. The early, very rapid first step involves the strictly intramolecular cleavage of the N-terminal regions of NS and IS1. The second, much slower step, which is likely to be intermolecular, releases these two peptides by cleavages in their C-terminal regions. Our data show that despite the difference in kinetics, these two steps cannot occur without Ca^{2+}. The similarities between the Ca^{2+} titration profiles of p94I-II and the homologous μI-II and mI-II strongly suggest that, as for the ubiquitous calpains, the catalytic triad of p94 is not aligned in its active conformation until Ca^{2+} binds to the core. Our results also corroborate that activation of p94 by Ca^{2+} involves not only realignment of its catalytic triad but also autolytic removal of the internal propeptide (IS1).

The dramatic effect of Ca^{2+} on both autolysis and proteolysis of exogenous substrates by the protease core of p94 documented in this study indicates that p94 is indeed a Ca^{2+}-dependent protease. Traces of autolysis observed in the presence of EDTA, with or without NaCl, should not be misconstrued as Ca^{2+} independency. Rather, they reflect the presence of trace amounts of Ca^{2+} present in stock solutions and the ability of the enzyme to compete for these ions with the chelating agent. Our data revealed that p94I-II undergoes a substantial conformational change upon Ca^{2+} binding which is characteristic of the proteolytic cores of μ- and m-calpain (*5*, *25*). This work with the protease core of p94 supports the hypothesis that the fundamental Ca^{2+} dependency of this family lies within the proteolytic core.

ACKNOWLEDGMENT

We are very grateful to Dr. Tudor Moldoveanu and Dominic Cuerrier for comments on the manuscript.

REFERENCES

1. Sorimachi, H., and Suzuki, K. (2001) The structure of calpain, *J. Biochem. 129*, 653−64.
2. Goll, D., Thompson, V., Li, H., Wei, W., and Cong, J. (2003) The calpain system, *Physiol. Rev. 83*, 731−801.
3. Hosfield, C. M., Elce, J. S., Davies, P. L., and Jia, Z. (1999) Crystal structure of calpain reveals the structural basis for Ca^{2+}-dependent protease activity and a novel mode of enzyme activation, *EMBO J. 18*, 6880−9.
4. Strobl, S., Fernandez-Catalan, C., Braun, M., Huber, R., Masumoto, H., Nakagawa, K., Irie, A., Sorimachi, H., Bourenkow, G., Bartunik, H., Suzuki, K., and Bode, W. (2000) The crystal structure of calcium-free human m-calpain suggests an electrostatic switch mechanism for activation by calcium, *Proc. Natl. Acad. Sci. U.S.A. 97*, 588−92.
5. Moldoveanu, T., Hosfield, C. M., Lim, D., Elce, J. S., Jia, Z., and Davies, P. L. (2002) A Ca^{2+} switch aligns the active site of calpain, *Cell 108*, 649−60.
6. Sorimachi, H., Imajoh-Ohmi, S., Emori, Y., Kawasaki, H., Ohno, S., Minami, Y., and Suzuki, K. (1989) Molecular cloning of a novel mammalian calcium-dependent protease distinct from both m- and mu-types. Specific expression of the mRNA in skeletal muscle, *J. Biol. Chem. 264*, 20106−11.
7. Sorimachi, H., Toyama-Sorimachi, N., Saido, T. C., Kawasaki, H., Sugita, H., Miyasaka, M., Arahata, K., Ishiura, S., and Suzuki, K. (1993) Muscle-specific calpain, p94, is degraded by autolysis immediately after translation, resulting in disappearance from muscle, *J. Biol. Chem. 268*, 10593−605.
8. Branca, D., Gugliucci, A., Bano, D., Brini, M., and Carafoli, E. (1999) Expression, partial purification and functional properties of the muscle-specific calpain isoform p94, *Eur. J. Biochem. 265*, 839−46.
9. Sorimachi, H., Saido, T. C., and Suzuki, K. (1994) New era of calpain research. Discovery of tissue-specific calpains, *FEBS Lett. 343*, 1−5.
10. Ma, H., Fukiage, C., Azuma, M., and Shearer, T. R. (1998) Cloning and expression of mRNA for calpain Lp82 from rat lens: Splice variant of p94, *Invest. Ophthalmol. Visual Sci. 39*, 454−61.
11. Herasse, M., Ono, Y., Fougerousse, F., Kimura, E., Stockholm, D., Beley, C., Montarras, D., Pinset, C., Sorimachi, H., Suzuki, K., Beckmann, J. S., and Richard, I. (1999) Expression and functional characteristics of calpain 3 isoforms generated through tissue-specific transcriptional and posttranscriptional events, *Mol. Cell. Biol. 19*, 4047−55.
12. Azuma, M., Fukiage, C., Higashine, M., Nakajima, T., Ma, H., and Shearer, T. R. (2000) Identification and characterization of a retina-specific calpain (Rt88) from rat, *Curr. Eye Res. 21*, 710−20.
13. Nakajima, T., Fukiage, C., Azuma, M., Ma, H., and Shearer, T. R. (2001) Different expression patterns for ubiquitous calpains and Capn3 splice variants in monkey ocular tissues, *Biochim. Biophys. Acta 1519*, 55−64.
14. De Tullio, R., Stifanese, R., Salamino, F., Pontremoli, S., and Melloni, E. (2003) Characterization of a new p94-like calpain form in human lymphocytes, *Biochem. J. 375*, 689−96.
15. Kawabata, Y., Hata, S., Ono, Y., Ito, Y., Suzuki, K., Abe, K., and Sorimachi, H. (2003) Newly identified exons encoding novel variants of p94/calpain 3 are expressed ubiquitously and overlap the α-glucosidase C gene, *FEBS Lett. 555*, 623−30.
16. Ma, H., Shih, M., Hata, I., Fukiage, C., Azuma, M., and Shearer, T. R. (1998) Protein for Lp82 calpain is expressed and enzymatically active in young rat lens, *Exp. Eye Res. 67*, 221−9.
17. Ma, H., Shih, M., Fukiage, C., Azuma, M., Duncan, M. K., Reed, N. A., Richard, I., Beckmann, J. S., and Shearer, T. R. (2000) Influence of specific regions in Lp82 calpain on protein stability, activity, and localization within lens, *Invest. Ophthalmol. Visual Sci. 41*, 4232−9.
18. Ono, Y., Kakinuma, K., Torii, F., Irie, A., Nakagawa, K., Labeit, S., Abe, K., Suzuki, K., and Sorimachi, H. (2004) Possible regulation of the conventional calpain system by skeletal muscle-specific calpain, p94/calpain 3, *J. Biol. Chem. 279*, 2761−71.
19. Anderson, L. V., Davison, K., Moss, J. A., Richard, I., Fardeau, M., Tome, F. M., Hubner, C., Lasa, A., Colomer, J., and Beckmann, J. S. (1998) Characterization of monoclonal antibodies to calpain 3 and protein expression in muscle from patients with limb-girdle muscular dystrophy type 2A, *Am. J. Pathol. 153*, 1169−79.
20. Baghdiguian, S., Martin, M., Richard, I., Pons, F., Astier, C., Bourg, N., Hay, R. T., Chemaly, R., Halaby, G., Loiselet, J., Anderson, L. V., Lopez de Munain, A., Fardeau, M., Mangeat, P., Beckmann, J. S., and Lefranc, G. (1999) Calpain 3 deficiency is associated with myonuclear apoptosis and profound perturbation of the IκBα/NF-κB pathway in limb-girdle muscular dystrophy type 2A, *Nat. Med. 5*, 503−11.
21. Kinbara, K., Ishiura, S., Tomioka, S., Sorimachi, H., Jeong, S. Y., Amano, S., Kawasaki, H., Kolmerer, B., Kimura, S., Labeit, S., and Suzuki, K. (1998) Purification of native p94, a muscle-specific calpain, and characterization of its autolysis, *Biochem. J. 335* (Part 3), 589−96.
22. Rey, M. A., and Davies, P. L. (2002) The protease core of the muscle-specific calpain, p94, undergoes Ca^{2+}-dependent intramolecular autolysis, *FEBS Lett. 532*, 401−6.
23. Diaz, B. G., Moldoveanu, T., Kuiper, M. J., Campbell, R. L., and Davies, P. L. (2004) Insertion sequence 1 of muscle-specific calpain, p94, acts as an internal propeptide, *J. Biol. Chem. 279*, 27656−66.
24. Kunkel, T. A., Bebenek, K., and McClary, J. (1991) Efficient site-directed mutagenesis using uracil-containing DNA, *Methods Enzymol. 204*, 125−39.
25. Moldoveanu, T., Hosfield, C. M., Lim, D., Jia, Z., and Davies, P. L. (2003) Calpain silencing by a reversible intrinsic mechanism, *Nat. Struct. Biol. 10*, 371−8.
26. Dutt, P., Spriggs, C. N., Davies, P. L., Jia, Z., and Elce, J. S. (2002) Origins of the difference in Ca^{2+} requirement for activation of mu- and m-calpain, *Biochem. J. 367*, 263−9.

BI051917J